

# The Mixing Character within Oxidation Reactor in Titanium Dioxide Production by Chloride Process

Fengyang Chen<sup>1,2,a</sup>, Ping Lu<sup>1,2</sup>, Dongqin Li<sup>1,2</sup>, Yadong Li<sup>b,3</sup>, Yanqing Hou<sup>c,4</sup>,  
Gang Xie<sup>5</sup>, Ni Yang<sup>5,d</sup>, Lin Tian<sup>5</sup>

<sup>1</sup>State Key Laboratory of Vanadium and Titanium Resources Comprehensive Utilization Panzhihua, China

<sup>2</sup>Faculty of Metallurgical and Energy Engineering, Kunming University of Science and Technology Kunming, China

afychen@stu.kust.edu.cn

<sup>3</sup>Faculty of Metallurgical and Energy Engineering, Kunming Metallurgy College Kunming, China

bcancanyjs@sina.com

<sup>4</sup>State Key Laboratory of Complex Nonferrous Metal Resources Clean Utilization, Kunming University of Science and Technology Kunming, China

chhouyanqing@163.com

<sup>5</sup>Kunming Metallurgical Research Institute Kunming, China

dyangnihejie@126.com

**Abstract.** Chloride process is cost effective and environmental benefit, and the  $TiCl_4$  oxidation is the most important stage in this process. The structure of the jet ring has an obviously effect on the mixing of  $TiCl_4$  and  $O_2$  in the oxidation reactor, which is the key equipment in the production of titanium pigment. In this paper, the gas mixing condition with five jet rings of different structure was simulated and analyzed by computational fluid dynamics (CFD) simulation. The radial concentration distribution of  $TiCl_4$  and the non-uniformity of the mixture with different jet rings were obtained. The results showed the structure of the jet ring has great effect on the gas mixing. The mixing condition of the jet ring with combined opening orifice is better than that of the jet ring with uniform opening orifice, which is more effective in realizing fast and uniform mixing condition of  $TiCl_4$  and  $O_2$ .

**Keywords:** Oxidation Reactor; Computational Fluid Dynamics; Jet in Crossflow; Jet Ring Structure; Non-uniformity

## 1. Introduction

Titanium dioxide is an important inorganic pigment with non-toxic, best whiteness, highest refractive index, best covering power and brightness, and is considered to be the best performing white pigment in the world [1]. The application of  $TiO_2$  covers almost all industrial fields and daily life products, it is an indispensable and important raw material for the production of coatings, plastics, rubber, chemical fiber, ink, paper, metallurgy, daily chemical, medicine, food, cosmetics and other industries [2,3]. With the progress of science and technology and the improvement of people's living standards in China, the demand for titanium dioxide is also growing. 215,000 tons of titanium dioxide were imported nationwide in 2017, an increase of 7.5% year-on-year; 198,000 tons of titanium dioxide were imported nationwide in 2018; and 216,000 tons were imported in 2019, an increase of 11.3% year-on-year [4-6]. At present, the main methods for producing high-grade rutile titanium dioxide are sulfuric acid and chlorination methods. China is the largest country in the production of titanium dioxide by sulfuric acid method, and the technology is the most mature. However, the key technology for the production of titanium dioxide by the chlorination method is controlled by only a few foreign companies, and only a few domestic enterprises have introduced the technology [1]. The chlorination method has become the mainstream technology and development trend of the international titanium dioxide industry with its advantages of short

process, few procedures, easy expansion of production capacity, high product quality, low pollution, and high degree of automation [7].

TiCl<sub>4</sub> vapor phase oxidation reactor is the core technology and equipment in the titanium dioxide chlorination process. The reaction of  $\text{TiCl}_4 + \text{O}_2 = \text{TiO}_2 + 2\text{Cl}_2$  occurs in the oxidation reactor, and the reaction rate in this process is extremely rapid. If the two reactants are not mixed quickly and evenly enough, the reaction rate in the reaction zone will be uneven, thus leading to a wide particle size distribution of the resulting titanium dioxide, making the product quality unqualified. In addition, since the reaction is exothermic, the inhomogeneity of the mixture can lead to excessive concentration of heat, which in turn can lead to sintering and scarring. This is why the intensive mixing of the reactants is particularly important. Therefore, the gas mixing rate must be studied in detail to reveal the hydrodynamic characteristics of the feed gas in the reactor. Most of the feed rings used in industry achieve rapid mixing of reactants with cross jets. Zhang [8] analyzed the gas mixing and reaction process by cold and hot mode tests, and Lin proposed to simulate the TiCl<sub>4</sub> gas-phase oxidation course by the process of physical quantity change of titanium dioxide particle size growth, while Zhang suggested that the inlet ring should preferably take a tangential approach to improve the gas mixing effect. Lv et al. [9] used tracer method and particle image velocimetry (PIV) for experimental study of gas-phase mixing, respectively, and found that the main factors affecting its mixing effect are the momentum ratio and intersection angle of the two streams, but the specific key technical indicators such as momentum ratio, intersection angle and jet ring opening position were still in disagreement. Li et al. [10] used the momentum theorem to theoretically derive the pressure distribution law for variable masses in annular channels, and Lv [11] used a simplified one-dimensional model for an approximate theoretical analysis of the static pressure distribution law for variable mass flow in annular channels. The momentum exchange coefficients introduced in these models need to be determined experimentally, but the data on momentum exchange coefficients needed in engineering are scarce and the flow structure of the fluid in the annular channel is not clear. Singh [12] investigated the interaction between methane/air flame and TiCl<sub>4</sub> oxidation for TiO<sub>2</sub> synthesis by two-dimensional direct numerical simulations based on a multi-step chemical reaction mechanism. Sung et al. [13] used a maelstrom dissipation method to simulate the TiO<sub>2</sub> nucleation process. Schild et al. [14] used particle growth kinetics to simulate the chemical reactions and particle formation kinetics during TiO<sub>2</sub> formation. Recently, Buddhiraju [15] et al. have simulated the formation of TiO<sub>2</sub> nanoparticles in turbulent reactions using a fully coupled model and a flame dynamics-monodisperse population equilibrium coupling model, respectively.

Although researchers have obtained some research results on the gas flow in the feed ring, there is still disagreement on the key technical specifications such as specific momentum ratio, intersection angle and jet ring opening position. In order to obtain the best effect of gas mixing, this paper investigates the effect of jet ring structure on the fluid mixing effect by using computational fluid (CFD) software to provide a reference for the design and optimization of the feed ring.

## 2. Establishment of Model

### 2.1 Geometric Model of Oxidation Reactor

The industrial titanium dioxide oxidation reactor by chlorination is very complex, and the geometric model developed for the simulations in this paper is simplified to some extent without affecting the study of gas mixing. As shown in Fig. 1, the high-temperature oxygen stream exits the combustion chamber and flows uniformly into the

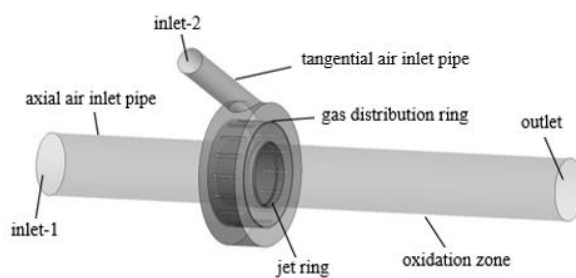


Fig. 1. Structure of the Oxidation Reactor.

mixing zone through the axial inlet tube (inlet-1). The preheated titanium tetrachloride vapor enters through the tangential inlet tube (inlet-2), passes through the gas distribution ring for uniform distribution, and then passes through the jet ring and is sprayed radially into the high-temperature oxygen cross-stream at high speed and mixed with it.

## 2.2 Governing Equation

The mixing process of high-temperature O<sub>2</sub> and TiCl<sub>4</sub> steam in the oxidation reactor is very complex, and to characterize its flow accurately, the continuity equation, momentum equation, turbulent kinetic energy and turbulent kinetic energy dissipation rate equations of the fluid flow must be described simultaneously. In this paper, the mixing of O<sub>2</sub> and TiCl<sub>4</sub> gas under steady-state conditions is simulated with the following 2 assumptions: (1) the gas flow has reached a steady state, disregarding the O<sub>2</sub> and TiCl<sub>4</sub> flow into the annulus at the starting and ending; (2) the system is pure O<sub>2</sub> and TiCl<sub>4</sub> gas without considering the impurities and chemical reactions in it. In the steady state, the control equations are described in the literature [16].

## 2.3 Boundary Conditions and Numerical Analysis Methods

ANSYS Fluent 14.5.0 was used to solve the calculations, and the calculation model was a three-dimensional oxidation reactor with tangential inlet. The mesh accuracy and quality meet the research requirements and do not cause calculation errors. Realizable k-ε turbulence model is used for the flow field model. The steady-state solution method of SIMPLEC algorithm is used for the pressure and velocity coupling, and the default relaxation factor in Fluent is used. The Standard Difference Scheme is used for the pressure equation, and the Second-order Upwind Difference Scheme is used for the solution of the momentum, turbulent kinetic energy, and turbulent kinetic energy dissipation rate equations. The residuals of the continuity equation, momentum equation, turbulent kinetic energy and turbulent kinetic energy dissipation rate equations are all 10<sup>-3</sup>, and the computational results are converged.

The boundary conditions are set as follows:

- (1) Inlet boundary conditions: choose velocity inlet boundary, set as Table I .
- (2) Outlet boundary conditions: the outlet is set as pressure outlet, using the default settings in Fluent.

TABLE 1. INLET BOUNDARY CONDITIONS

Air inlet	Material	Temperature (m/s)	Velocity (m/s)	Turbulence intensity(%)	Hydraulic diameter(m)
inlet-1	O <sub>2</sub> (g)	1773	7.24	3.91	0.2
inlet-2	TiCl <sub>4</sub> (g)	700	19.56	6.34	0.08

TABLE 2. STRUCTURE OF JET RING

Number	Opening structure	Aperture(m)	Hole number
Case #1	Uniform openings	0.018	12
Case #2	Uniform openings	0.013	24
Case #3	Uniform openings	0.009	48
Case #4	Slit openings	0.005	slit
Case #5	Combined openings	0.009&0.013	24&12

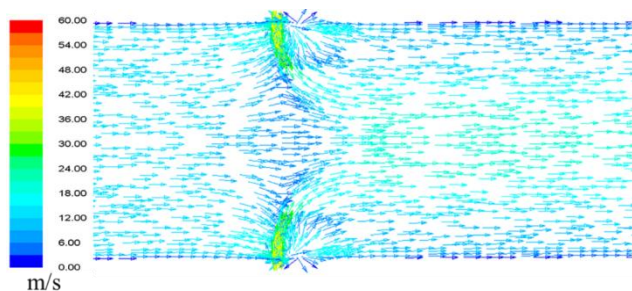


Fig. 2. Velocity Vector of Jet Mixing in the Reaction Chamber.

### 3. Result and Discussion

In this paper, five different structures of jet rings were studied, and their structural parameters are listed in Table II. The jet rings with different opening structures keep the same total area of openings, but the number of openings and the size of the openings vary, where the ring slit openings are equivalent to closely arrange the openings according to the minimum opening diameter.

#### 3.1 Jet Mixing Flow Field Analysis

Fig. 2 shows the velocity distribution vector diagram of TiCl<sub>4</sub> jet mixed with O<sub>2</sub> crossflow in the reaction tube on a cross section with a jet orifice in Case #1. The flow field distribution in the other Cases has a similar situation to that in Case #1. As can be seen in Fig. 2, the TiCl<sub>4</sub> jet is injected from the jet orifice into the O<sub>2</sub> crossflow in the reaction tube. The lateral O<sub>2</sub> main stream is obstructed by the TiCl<sub>4</sub> jet to form a flow around. Under the effect of the flow around, the perimeter pressure distribution of the TiCl<sub>4</sub> jet is asymmetric when comparing the front with the back, and thus the TiCl<sub>4</sub> jet is bent by the thrust of the O<sub>2</sub> crossflow. When the transverse turbulent jet forms a stable flow state, the whole jet development can be divided into three zones: (I) the potential flow core zone, which is in the center of the jet at the outlet of the jet hole. The TiCl<sub>4</sub> jet in this zone is little influenced by the O<sub>2</sub> crossflow, the jet bends less, and the flow direction is basically along the direction of the initial injection of the TiCl<sub>4</sub> jet. However, the length of the potential core zone is shortened compared to the jet injected into the stationary atmosphere. (II) The maximum deformation zone, at the end of the core area of the potential flow, the transverse pressure gradient is large, the doping effect is strong, the flow velocity decays faster, and the flow direction of the main body of the TiCl<sub>4</sub> jet is obviously deflected and finally parallel to the O<sub>2</sub> crossflow. (III) Far flow field area, after the maximum deformation area, the direction of TiCl<sub>4</sub> jet basically tends to be the same as that of O<sub>2</sub> cross-flow, the jet has been fully developed, the effect of flow around of O<sub>2</sub> cross-flow basically disappears, and the influence of the jet on the main flow field gradually weakens.

#### 3.2 Effect of Jet Ring Opening Structure on Concentration Distribution

Figure 3 shows the radial concentration distribution of TiCl<sub>4</sub> gas in the reaction tube at the cross sections of 0.04m, 0.08m, 0.12m and 0.16m from the jet hole under five different structures of jet

rings. The horizontal coordinate ( $r/R$ ) is the radial relative position of the measurement point from the wall of the reaction tube, and the vertical coordinate ( $c_i/c_m$ ) is the relative concentration of  $TiCl_4$  in the reaction tube ( $c_i$  is the concentration of the  $i$ th measurement point, and  $c_m$  is the average value of the concentration on the cross section where the measurement point is located). As can be seen from the figure, the radial concentration distribution of  $TiCl_4$  differs significantly for the jet ring with different opening structures. The number of openings in the jet ring in Case #1 is small, the aperture diameter is larger, and the concentration distribution of  $TiCl_4$  in the center of the tube is larger. While in Case #2, the  $TiCl_4$  maximum concentration point starts to shift toward the tube wall ( $r/R = \pm 0.5$ ). In Case #3, the number of jet ring openings is large, the diameter of the openings is smaller, and the  $TiCl_4$  concentration is lowest in the center of the tube and higher near the tube wall. In the slit-opened and combined-opened jet rings Case #4 and Case #5, the  $TiCl_4$  concentration is also relatively low in the center of the tube, but the value higher than Case #3, and the highest point of concentration is also close to the tube wall. The radial relative concentration distribution of  $TiCl_4$  becomes more uniform in all five jet rings as the distance from the jet hole gets farther. In Case #1, Case #2 and Case #3, the  $TiCl_4$  radial relative concentration distribution curve becomes relatively flat at a cross-sectional distance of 0.16m from the jet hole, and a distance of at least 0.12m is also required in Case #4. However, in Case #5, the concentration distribution curve is nearly straight at a cross-sectional distance of 0.08m from the jet hole, and the distance required for homogeneous mixing is shorter, indicating that this Case is more favorable for rapid and homogeneous mixing of the  $TiCl_4$  jet and the  $O_2$  cross-stream.

It can also be seen from Fig. 3 that the radial concentration distribution of  $TiCl_4$  gas in the reaction tube is very non-uniform in Case #1, Case #2 and Case #3 at the cross-sectional distance of 0.04m from the jet hole. And the inhomogeneity of the initial  $TiCl_4$  concentration distribution in the slit-opened jet ring Case #4 was reduced, but it is still unavoidable. However, in the combined open-hole jet ring Case #5, the relative  $TiCl_4$  concentration distribution curve has been smoothed and the uniformity and the initial concentration distribution has been greatly improved. To illustrate this uniformity of initial concentration distribution more visually, Fig. 4 shows the radial concentration distribution of  $TiCl_4$  gas in the reaction tube at a cross-sectional distance of 0.04m from the jet hole for these five different structured jet rings. As can be seen in Fig. 4, the curve of the initial distribution of  $TiCl_4$  concentration in Case #5 is the flattest, i.e., the best uniformity of the initial distribution of concentration, which is consistent with the conclusion analyzed in Fig. 3 above.

In cross-jet mixing, convective diffusion, turbulent diffusion and molecular diffusion act simultaneously to mix the fluid [10]. The small holes in the jet ring split the  $TiCl_4$  fluid into multiple jets, which enter the mainstream  $O_2$  and mix with it by convective diffusion. Further, the fluid forms smaller scale gas microclusters due to turbulent diffusion. Finally, the fluid achieves microscopic mixing uniformity by the effect of molecular diffusion. When the opening area of the jet ring is the same, the  $TiCl_4$  gas jet penetration ability is stronger with the jet ring with large holes, and the fluid can penetrate to the center of the tube, but due to the fluid gathering in the center of the tube will form a large scale mixing. While the jet ring with smaller apertures has a weaker jet penetration ability and cannot flow to the center of the tube by convective diffusion. The  $TiCl_4$  gas will flow in the direction of the mainstream  $O_2$ , and its flow direction will soon be deflected to follow the mainstream direction along the tube wall. This is not conducive to the mixing efficiency of  $TiCl_4$  and  $O_2$ . And the combined open-hole jet ring structure can reduce the inhomogeneity of the initial distribution of concentration.

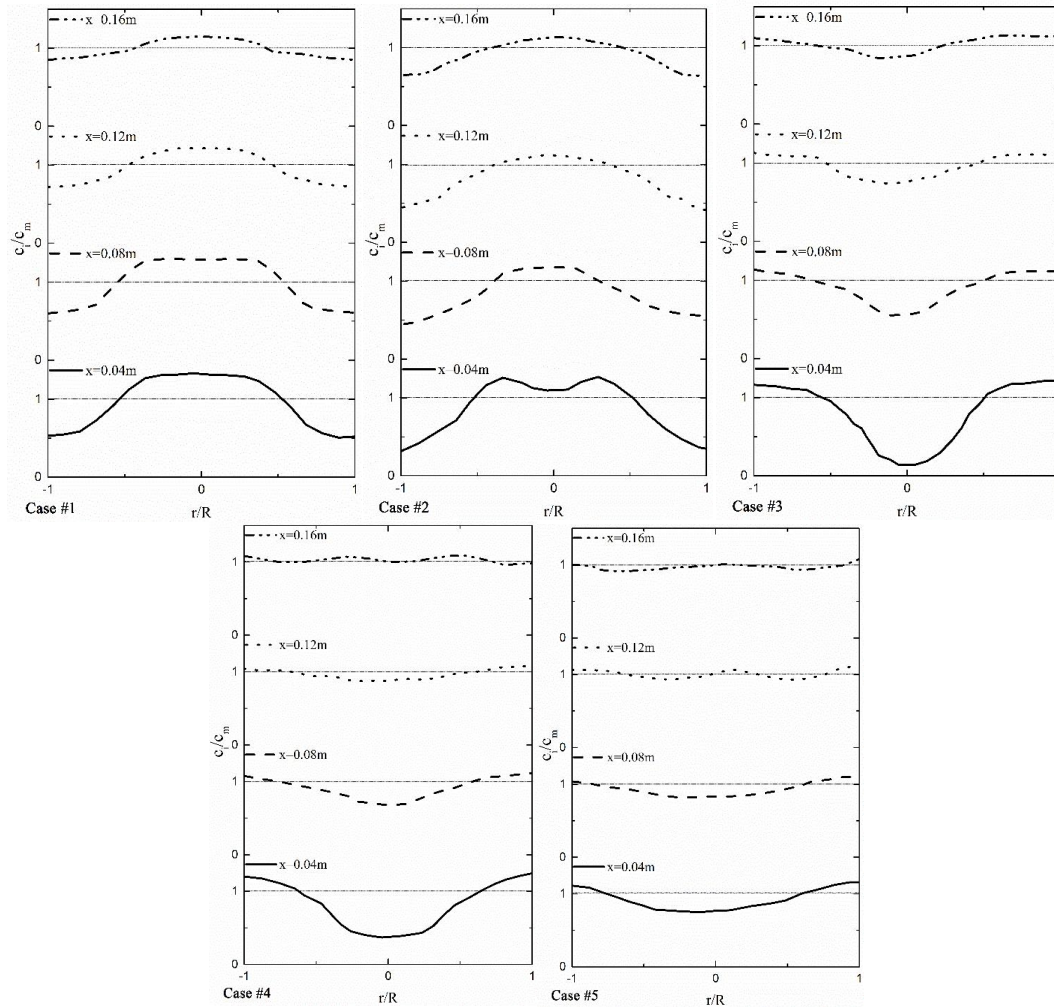


Figure 3. Radial Concentration Distribution of TiCl4 with Five Different Jet Rings.

### 3.3 Mixing Inhomogeneity

In order to illustrate the gas mixing effect under the above five jet ring structures more accurately, the inhomogeneity  $M$  is introduced, as shown in (1). A smaller value of the inhomogeneity  $M$  represents a higher degree of homogeneity at the measured point.

$$M = \sqrt{\frac{1}{n} \sum_{i=1}^n \left( \frac{c_i - c_m}{c_m} \right)^2}$$

Where  $c_i$  is the concentration of the  $i$ th measurement point and  $c_m$  is the average value of the concentration on the cross section where the measurement point is located.

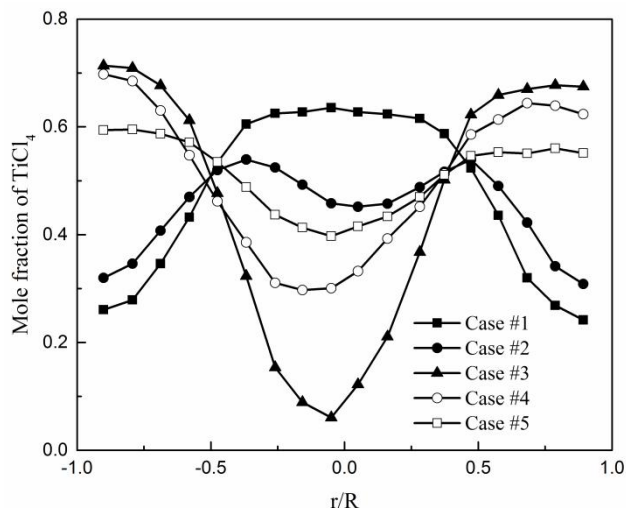


Figure 4. Radial Concentration Initial Distribution of TiCl4 with Different Jet Rings.

For the five types of jet ring structures, the M values of concentration inhomogeneity in the cross-section at 0.04m from the jet hole are 0.409, 0.185, 0.351, 0.242, and 0.114, respectively; and the M values of concentration inhomogeneity in the cross-section at 0.08m from the jet hole are 0.374, 0.126, 0.233, 0.106, and 0.048, respectively. The combination of open holes Case #5 of the jet ring has the smallest value of inhomogeneity, which is more conducive to rapid and uniform mixing of fluids. The concentration distribution of TiCl4 in the reaction tube has maximum and minimum points in all the above mentioned jet rings with different opening structures. The reason is that the penetration capacity of each jet is the same for the jet with uniform opening, and the uneven initial distribution of the fluid is inevitable. However, the combined open-hole Case #5 jet ring is used to control the initial distribution of the TiCl4 fluid jet by a reasonable combination of small holes of different apertures to better achieve rapid and uniform mixing of TiCl4 and O2.

#### 4. Conclusion

In the process of titanium dioxide production by chlorination, it is extremely important that the materials inside the oxidation reactor, TiCl4 and O2, are mixed quickly and uniformly. The structure of the jet ring opening is one of the important factors affecting the fluid mixing effect, and the following conclusions are drawn from the study of the effect of different structures of the jet ring on the mixing effect in this paper.

(1) In the oxidation reactor, TiCl4 and O2 are mixed in a cross-jet manner, and the initial inhomogeneity of fluid distribution is unavoidable when a jet ring with uniform opening structure is used. Designing and optimizing the jet ring open-hole structure makes TiCl4 and O2 mix rapidly and uniformly.

(2) Compared with the jet ring with uniform open-hole structure, the minimum value of inhomogeneity of initial distribution of TiCl4 gas concentration in the reaction tube is 0.114 under the jet ring structure with combined open-hole structure. Therefore, the initial distribution of TiCl4 fluid jet can be effectively controlled by the reasonable design of the jet ring with combined open-hole structure to facilitate the rapid and uniform mixing of TiCl4 and O2.

#### Acknowledgment

The authors are grateful to the National Natural Science Foundation of China Project (No. 21566015 and No. 52074141).

## References

- [1] Driel B.V., Artesani A. and Berg K., New insights into the complex photoluminescence behaviour of titaniumwhite pigments. *Dyes & Pigments*, 2018, 155: 138-146.
- [2] Romain B., Yu C., Phil T., et al. Characterisation of silicon, zirconium and aluminium coated titanium dioxide pigments recovered from paint waste. *Dyes and Pigments*, 2019, 162: 145-152.
- [3] Mansoor A., Fatimah A. and Marzie R., Preparation of titanium dioxide nanostructure from ilmenite through sulfate-leaching process and solvent extraction by D2EHPA, *Journal of the Iranian Chemical Society*, 2018, 15(11): 2533-2540.
- [4] Schubert D., Hertle S., Drummer D.. Influence of titanium oxide-based colourants on the morphological and tribomechanical properties of injection-moulded polyoxymethylene spur gears. *Journal of Polymer Engineering*, 2019, 39(8): 774-783.
- [5] Van Driel B.A., Kooyman P. J., Van den Berg K.J., Schmidt-Ott A., Dik J., A quick assessment of the photocatalytic activity of TiO<sub>2</sub> pigments-From lab to conservation studio!. *Microchem. J.*, 2016, 126: 162-171.
- [6] Driel B.A.V., Meer S. R.V. D., K.J.V.D. Berg, et al. Determining The Presence of Photocatalytic Titanium White Pigments via Embedded Paint Sample Staining: A Proof of Principle. *Studies in Conservation*, 2019, 64(5): 261-272.
- [7] Wang L.L., Li R.M., Sha J.Z., Hao B.R., Wang C.L.. Surface grafting modification of titanium dioxide by silane coupler KH570 and its influences on the application of blue light curing ink. *Dyes and Pigments*, 2019, 163: 232-237.
- [8] Zhang S M. Cold Analog Experiment for Chloride Process TiO<sub>2</sub> Production[J]. *Coating Industry*, 2000, (5): 20-22.
- [9] Lv Z M, Li C Z, Cong D Z, et al. Study on the mixing characteristics of the jet in the oxidation reactor for the preparation of titanium dioxide by chlorination[J]. *Chemical Engineering*, 2001,(03): 25-28.
- [10] Li R J, Chen Y H, Zhu Z B. Analysis on uniform fluid distribution of circle distributor in multitube fixed-bed reactor[J]. *Chemical Engineering*, 2009, 37(3): 20-26.
- [11] Lv Z M, Li C Z, Cong D Z. Gas Flow and Distribution in Circle Distributor[J]. *Chemical Engineering*, 2001, 29(2): 26-30.
- [12] Singh R, Raman V. Two-dimensional direct numerical simulation of nanoparticle precursor evolution in turbulent flames using detailed chemistry [J]. *Chemical Engineering Journal*, 2012, 207-208: 794-802.
- [13] Sung Y, Raman V, Fox R O. Large-eddy-simulation-based multiscale modeling of TiO<sub>2</sub> nanoparticle synthesis in aturbulent flame reactor using detailed nucleation chemistry [J]. *Chemical Engineering Science*, 2011, 66(19): 4370-4381.
- [14] Schild A, Gutsch A, Mühlenweg H, et al. Simulation of nanoparticle production in premixed aerosol flow reactors by interfacing fluid mechanics and particle dynamics [J]. *Journal of Nanoparticle Research*, 1999, 1(2): 305-315.
- [15] Buddhiraju V S, Runkana V. Simulation of nanoparticle synthesis in an aerosol flame reactor using a coupled flame dynamics–monodisperse population balance model [J]. *Journal of Aerosol Science*, 2012, 43(1): 1-13.
- [16] Shih T H, Liou W W, Shabbir A, et al. A New k-ε Eddy-Viscosity Model for High Reynolds Number Turbulent Flows-Model Development and Validation [J]. *Computers Fluids*, 1995, 24(3): 227–238.